Magnetic Memory from Site Isolated Dy(III) on Silica Materials

Florian Allouche, Giuseppe Lapadula, Georges Siddiqi, Wayne W. Lukens, Olivier Maury, Boris Le Guennic, Fabrice Pointillart, Jan Dreiser, Victor Mougel, Olivier Cador, et al.

HAL Id: hal-01480162
https://hal.sorbonne-universite.fr/hal-01480162

Submitted on 1 Mar 2017

Magnetic Memory from Site Isolated Dy(III) on Silica Materials

Florian Allouche,[†] Giuseppe Lapadula,[†] Georges Siddiqi,[†] Wayne W. Lukens,[‡] Olivier Maury,[§] Boris Le Guennic,[‖] Fabrice Pointillart,[‖] Jan Dreiser,[⊥] Victor Mougel,*[#] Olivier Cador,*[‖] and Christophe Copéret*[†]

[†]Department of Chemistry and Applied Biosciences, ETH Zürich, Vladimir Prelog Weg 1-5, CH-8093 Zürich, Switzerland

[‡]Chemical Sciences Division, Lawrence Berkeley National Laboratory, Berkeley, California 94720, United States

[§]Univ Lyon, Ecole Normale supérieure de Lyon, Laboratoire de Chimie UMR 5182 CNRS—Université Claude Bernard Lyon 1—ENS Lyon, 46 Allée d'Italie, 69364 Lyon Cedex 07, France

[‖]Institut des Sciences Chimiques de Rennes UMR 6226 CNRS-UR1, Université de Rennes 1, 35042 Rennes Cedex, France

[⊥]Swiss Light Source, Paul Scherrer Institute, CH-5232 Villigen PSI, Switzerland

[#]Laboratoire de Chimie des Processus Biologiques, CNRS UMR 8229, Collège de France, Université Pierre et Marie Curie, 11 Place Marcelin Berthelot, 75231 Paris Cedex 05, France

S Supporting Information

ABSTRACT: Achieving magnetic remanence at single isolated metal sites dispersed at the surface of a solid matrix has been envisioned as a key step toward information storage and processing in the smallest unit of matter. Here, we show that isolated Dy(III) sites distributed at the surface of silica nanoparticles, prepared with a simple and scalable two-step process, show magnetic remanence and display a hysteresis loop open at liquid ^{4}He temperature, in contrast to the molecular precursor which does not display any magnetic memory. This singular behavior is achieved through the controlled grafting of a tailored Dy(III) siloxide complex on

partially dehydroxylated silica nanoparticles followed by thermal annealing. This approach allows control of the density and the structure of isolated, "bare" Dy(III) sites bound to the silica surface. During the process, all organic fragments are removed, leaving the surface as the sole ligand, promoting magnetic remanence.
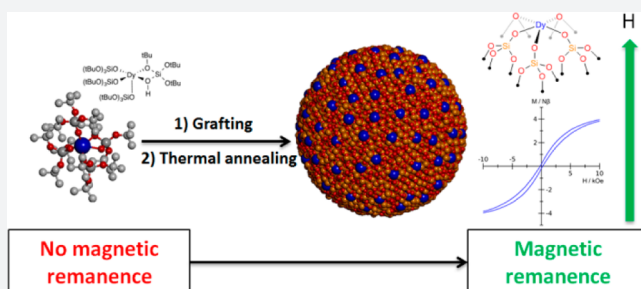
The pressure to increase information storage densities has grown tremendously during recent decades, which necessitates downsizing storage elements. Ultimately, the size of such an element is limited to a single atom. In that case, the magnetic moment originating from the atom's quantum mechanical spin could be used to encode bits of information. This goal, however, requires sufficient temporal stability of the magnetic moment, which is manifested in the appearance of magnetic remanence, i.e., the capability of a magnetic system to retain its magnetic moment after removal of the external, magnetizing field.

In this context, the discovery of single-molecule magnets (SMMs) has been a major breakthrough to envision data storage at the nanometer scale. SMMs are unique molecules in which the magnetic moment resists reorientation[1] in the absence of a magnetic field. The guideline of most studies on SMMs has been the quest for the most stable nanomagnet, i.e., the most coercive at the highest temperature.[2] However, most SMMs are produced and studied in the condensed crystalline phase in which the single magnetic molecules cannot be addressed one-by-one. To solve this problem, several strategies have been investigated in recent years aiming at the isolation of

atomic scale entities presenting magnetic remanence: heterogenization (surface immobilization) of SMMs[3] by grafting,[4−8] surface functionalization with organic ligands,[7,9] physisorption on a support,[10−12] supramolecular interactions,[13] or encapsulation[14,15] (Figure 1A,B), for example. However, these strategies present significant challenges. In particular, it is difficult to preserve the magnetic remanence behavior upon heterogenization as the SMM and the surface are produced separately and then assembled together. In other words, the properties of magnetic entities at the surface differ from the properties in the bulk or of individual molecular entities. Most of the SMMs are based on transition metals or f-elements and result from the combination of two key parameters: a large spin and a significant magnetic anisotropy. This anisotropy is a property of the metal center used, and its magnitude can be significantly modulated by its coordination sphere. Hence, heterogenization, which often changes the coordination sphere of the metal center, can significantly alter the required magnetic properties.
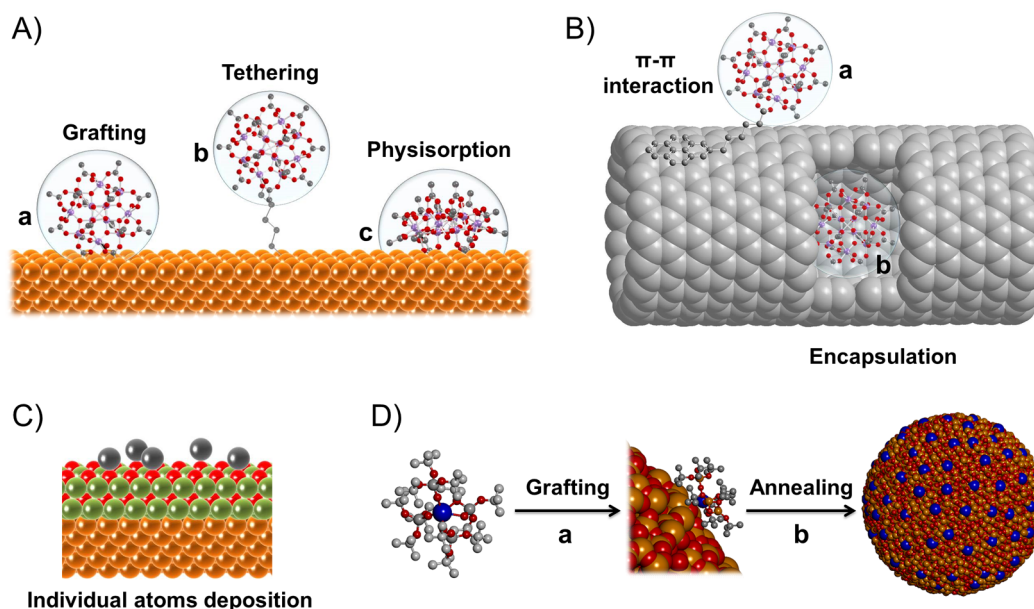
Figure 1. Immobilization strategies of single-molecule and single-atom magnets. (A) Immobilization of single-molecule magnets by grafting (a), through surface decoration with organic ligands (b), or by physisorption on the surface (c). (B) Immobilization on carbon nanotubes by supramolecular interaction (a) or encapsulation (b) (part of the nanotube wall is not represented for clarity). (C) Isolated atoms on flat metallic surface protected by an insulating decoupling layer. (D) Our strategy for immobilization of ions on metal oxide surfaces, based on a grafting step (a) and a thermolytic step (b).

As illustrated recently, single-atom deposition directly onto the surface is the ultimate size limit.[15] The magnetic remanence for single atoms of Ho on MgO/Ag(100) persists up to 30 K (Figure 1C).[16] This strategy showed unprecedented magnetic properties, but has limited thermal stability (the atoms being immobile only up to 50 K). Heterogenization on atomically flat surfaces has generated significant interest, as STM techniques enable manipulation of individual molecules or atoms. However, this approach requires complex techniques for the characterization of the materials. The development of strategies to rapidly screen the magnetic properties of the materials using conventional magnetometric techniques is thus highly desirable, but these techniques often fail when applied to flat surface analogues because of the small amount of magnetic material, which is only present at the surface. In that respect, we have demonstrated that the surface chemistry of a silica layer on passivated silicon wafers is analogous to that of high surface area silica nanoparticles and that identical surface species were found upon immobilization of molecules on both supports.[17,18]

On this basis and in view of the exceptional magnetic properties of lanthanide ions,[19−21] we targeted an approach to prepare a class of magnetic nanomaterials consisting of *isolated lanthanide ions at the surface of nonmagnetic nanoparticles*, which could then be applied to flat surfaces. Of all the challenges to be met to elaborate such a material, the thermal stability and the absence of organic ligands are of utmost importance. In particular, one would like to conceive a material that can be cycled between blocking temperatures and room temperature without any alteration of its magnetic properties. The approach would benefit from a simple, large-scale synthetic process. Toward this goal, we have developed a strategy for producing fully inorganic isolated lanthanide ions on a silica matrix.[22−24] Our approach combines the site isolation of silica partially dehydroxylated at 700 °C (so-called SiO_{2-700}, presenting an average of ca. 0.8 surface silanol per nm^2),[25] the unique magnetic properties of Dy(III) ions[26]—a Kramers ion with a

large moment and often exhibiting a significant magnetic anisotropy—and the thermolytic molecular precursor approach, which allows clean removal of organic ligands and generation of isolated metal ions in an anisotropic environment provided by the surface.[27−31]

We first prepared and characterized a Dy(III) molecular precursor bearing thermally labile $(tBuO)_3SiO^-$ ligands, $Dy[OSi(OtBu)_3]_3[\kappa^2\text{-HOSi(OtBu)}_3]$ (**1**).[24] Grafting of **1** (1.05 equiv/silanol or ca. 0.26 mmol g^{-1}) on SiO_{2-700} led to the formation of $[(\equiv Si-O)Dy[(OSi(OtBu)_3)_2(\kappa^2\text{-HOSi-}(OtBu)_3)]$, **1/SiO₂** (Figure 2A). Treatment of **1/SiO₂** at 400 °C under high vacuum (10^{-5} mbar) afforded the fully inorganic material **Dy@SiO₂** as a white solid. The entire process can be carried out on gram scale. The absence of organic ligands in **Dy@SiO₂** was confirmed by FTIR spectroscopy, which shows the disappearance of $\nu(C-H)$ bands and the reappearance of isolated silanol bands upon thermal treatment (Figure 2B), similarly to what was observed for the corresponding Cr(II), Cr(III), and W(VI) analogues[29−31] used as single-site catalysts. The nature of the Dy sites in **1/SiO₂** and **Dy@SiO₂** was determined by X-ray absorption near edge structure (XANES) spectroscopy at the Dy L_{III}-edge. All Dy species (**1**, **1/SiO₂** and **Dy@SiO₂**) have similar edge energies (Figure 2C), indicating that during grafting of **1** and thermal decomposition of **1/SiO₂** the Dy oxidation state remains +III, with no evidence of metallic Dy.[32] The extended X-ray absorption fine structure (EXAFS) analysis at the Dy L_{III}-edge confirmed that, upon grafting **1** onto SiO_2, the coordination sphere is largely unchanged, with one $(tBuO)_3SiO^-$ ligand being replaced by a surface silanol moiety while retaining a chelating κ^2 neutral silanol ligand. Thermal treatment resulted in larger changes in the Dy coordination sphere. The best fit to the EXAFS spectrum of **Dy@SiO₂** is obtained by adding two neutral oxygen ligands at 2.42 Å to the three short oxygen neighbors at 2.20 Å. Those two additional oxygen atoms are presumably due to siloxane (Si–$\underline{O}$–Si) oxygens interacting with the metal
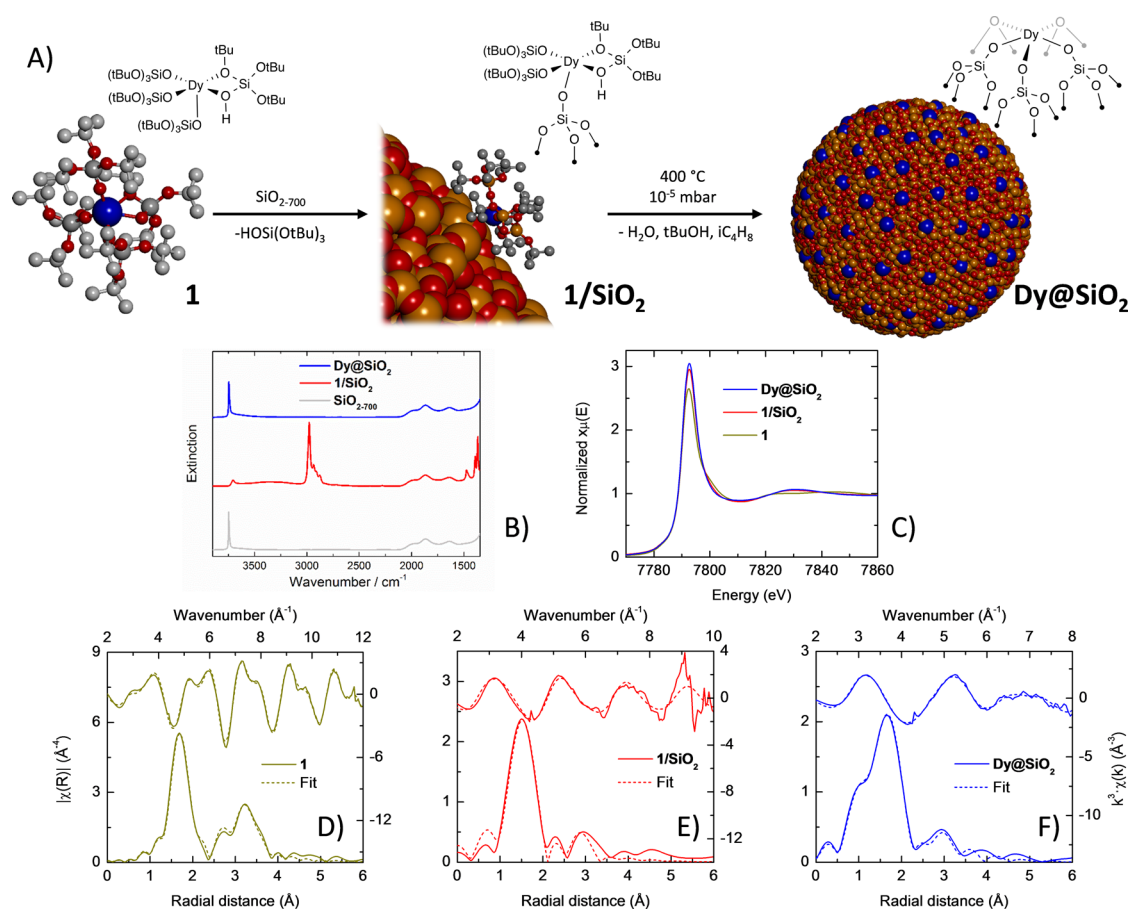
Figure 2. (A) Grafting of **1** on SiO_{2-700} to form **1/SiO₂** followed by a thermal annealing under high vacuum yielded **Dy@SiO₂** (color code: carbon (gray), silicon (orange), oxygen (red), and dysprosium (blue)). (B) FTIR transmission spectra of SiO_{2-700}, **1/SiO₂**, and **Dy@SiO₂**. Grafting of **1** (1.05 equiv/silanol or ca. 0.26 mmol g⁻¹) on SiO_{2-700} leads to the disappearance of most isolated silanols while a broad band appears at 3650 cm⁻¹, consistent with the presence of unreacted silanols interacting with organic ligands. (C) Dy L_{III}-edge XANES of **1**, **1/SiO₂**, and **Dy@SiO₂**. (D) k^3 weighted EXAFS fits in k-space (top) and R-space (bottom) of **1**. The fit of **1** includes five O atoms in the first coordination sphere: three at 2.11 Å, and one each at 2.39 and 2.53 Å. (E) k^3 weighted EXAFS fits in k-space (top) and R-space (bottom) of **1/SiO₂**. Aside from a shortening of the Dy–O paths of the κ^2 neutral silanol at 2.26 and 2.40 Å compared to the molecular structure, the structure of **1/SiO₂** is similar to **1** (Figures S4 and S5, Table S3). (F) k^3 weighted EXAFS fits in k-space (top) and R-space (bottom) of **Dy@SiO₂**. The best fit was obtained by including five O ligands, three with short (2.20 Å) and two with longer (2.42 Å) Dy–O distances (Figures S4 and S6, Table S3).

center. Taking into account such additional ligands is necessary for a good fit of the EXAFS spectra of **Dy@SiO₂**. In contrast, the EXAFS results show no Dy–Dy scattering paths, consistent with site isolation and with the coordination of the Dy(III) sites in **Dy@SiO₂** solely to the surface (Figure 2F and Table S3). Overall, EXAFS shows that Dy in **Dy@SiO₂** is bound to only 5 oxygen atoms and is therefore coordinatively unsaturated. The oxygen ligands arise from the surface and should therefore impose a very asymmetric environment. In fact, 1,10-phenanthroline, a bidentate ligand, coordinates to Dy as evidenced by a shift of the aromatic ring (C=C and C=N) in IR (Figure S17),[33] thus showing that Dy was not incorporated in the bulk of the material similarly to what was observed for Cr and Yb.[23,30]

Magnetic analyses of **1/SiO₂** and **Dy@SiO₂** provide room temperature $\chi_M T$ of 13.5 and 12.4 cm³ K mol⁻¹ respectively,[34] in agreement with the expected value of 14.2 cm³ K mol⁻¹ for the $^6H_{15/2}$ multiplet ground state of Dy(III) ions (Figures S7 and S8). The $\chi_M T$ values decrease on cooling with the thermal depopulation of M_J states to reach 11 and 10.4 cm³ K mol⁻¹ at 2 K. The saturation magnetizations at 2 K (4.6 and 4.5 Nβ for **1/SiO₂** and **Dy@SiO₂**, respectively) are consistent with the

stabilization of the $m_J = \pm 15/2$ Kramers doublet state well isolated from the first excited Kramers doublet (Figures S7 and S8). Ac susceptibility measurements performed in zero external dc field for **1/SiO₂** and **Dy@SiO₂** show that the magnetic moments of Dy(III) ions relax independently below 16 K at the nanoparticle surface, which is not the case for the molecular precursor **1**. Plots of the in phase (χ_M') and out of phase (χ_M'') ac magnetic susceptibilities in zero dc field as a function of frequency in the 2−18 K range (Figures 3A and S9) illustrate the slowdown of the magnetic relaxation and confirm that Dy(III) ions behave as magnets. These results indicate that the oxide surface can be viewed as the ligand that dictates the electronic properties of the Dy(III) ions. **Dy@SiO₂** relaxes more slowly than **1/SiO₂** at all temperatures and is therefore a more persistent magnet in zero field. At 2 K the relaxation time determined using an extended Debye model (Figure S10, Tables S4 and S5) is 100 times slower in **Dy@SiO₂** than in **1/SiO₂**. The high frequency limit (χ_S) corresponding to the nonrelaxing fraction of the magnetic susceptibility was fixed at zero to minimize free parameters. τ obeys the Arrhenius law above 9 K with an activation energy of 65($\pm$3) K (Table S4, Figure S11, see Materials and Methods for details) for
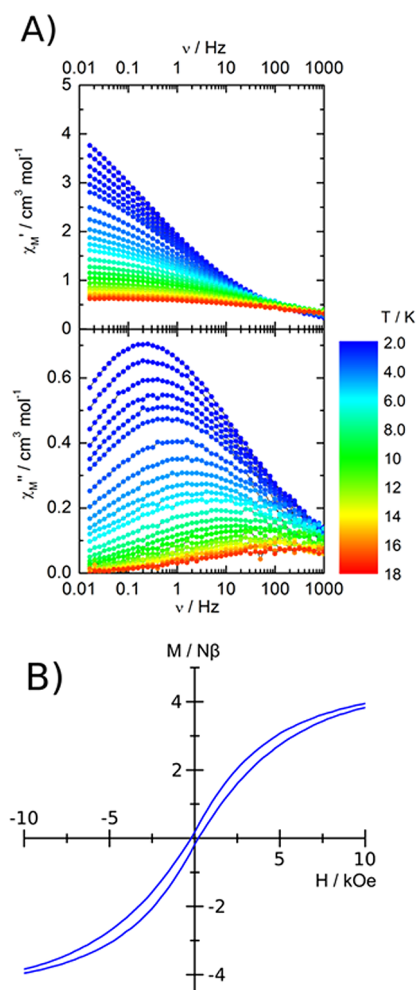
Figure 3. (A) Frequency dependence of the two components (χ_M' and χ_M'') of the ac susceptibility for **Dy@SiO$_2$** measured between 2 and 18 K in the absence of an external dc field. (B) Hysteresis loop for **Dy@SiO$_2$** measured at 2 K and at a sweep rate of 16 Oe s^{-1}.

Dy@SiO$_2$ while the activation energy (16($\pm$1) K, Table S5 and Figure S11) is much lower in **1/SiO$_2$**. At low temperature, the average relaxation time reaches a maximum at 1 s (Figure 3A) in **Dy@SiO$_2$**. Saturation of the relaxation time, which is commonly observed in Dy(III)-based SMMs,[35] prevents the storage of information at zero field. However, in the present case, a non-negligible fraction of Dy centers relaxes at time scale longer than 100 s due to the relatively large distribution of the relaxation times (Figure 3A, Table S4), which produces a hysteresis loop open at zero field between 2 and 5 K (Figures 3B and S12) in sweeping the field at 16 Oe s^{-1}. The same hysteresis loop closes when the sweep rate is decreased down to 0.6 Oe s^{-1} and remains slightly opened at intermediate rate of 2.5 Oe s^{-1} (Figure S13a). It must be mentioned that the loops close at high field (Figure S13b). The relaxation time in **Dy@SiO$_2$** is almost unaffected by an external dc field (Figure S14). On the contrary, the application of a moderate field on **1/SiO$_2$** slows down the relaxation time by a factor 100 (Figure S15) at 2 K, which causes the opening of a butterfly like hysteresis (Figure S16). This difference might originate from the higher number of vibration/rotation modes resulting from the presence of organic ligands in **1/SiO$_2$** with respect to its fully inorganic and more rigid counterpart **Dy@SiO$_2$**.

In contrast to traditional SMM heterogenization strategies where the magnetic properties of the molecular precursor are transferred to the surface, the magnetic memory properties of **Dy@SiO$_2$** appear only after grafting and thermal decomposition in our approach. This behavior most likely arises from the formation of highly constrained surface species and geometries that could not be obtained with molecular materials, thus illustrating the potential of the thermolytic precursor approach. Furthermore, thermolysis produces a non-centrosymmetric environment in **Dy@SiO$_2$**, with low coordinated Dy(III) exposed at the material surface as shown by EXAFS and 1,10-phenanthroline probe experiment (vide supra).

The strategy used here enabled the simple generation of fully inorganic isolated Dy(III) ions on a silica matrix, which is thermally stable up to at least 400 °C and behaves as isolated SMMs at liquid ^{4}He temperatures. The magnetic remanence of Dy sites in **Dy@SiO$_2$** depends solely on the site isolation on silica and is not found in the corresponding molecular entities, likely resulting from the unusual coordination environment of surface sites and the absence of ancillary organic ligand. The synthetic approach developed here is easily amenable to large scale production and is transferable to any type of oxide surfaces including layers of ferromagnetic oxides or oxide layers on wafers. It thus opens new avenues to generate and manipulate lanthanide nanomagnets for data storage at the nanoscale and quantum information processing.

■ ASSOCIATED CONTENT

Ⓢ Supporting Information

The Supporting Information is available free of charge on the ACS Publications website at DOI: 10.1021/acscentsci.7b00035.

Synthesis and characterization, IR, solution NMR, XRD data, XAS, and SQUID details (PDF)

■ AUTHOR INFORMATION

Corresponding Authors
*E-mail: ccoperet@ethz.ch.
*E-mail: olivier.cador@univ-rennes1.fr.
*E-mail: victor.mougel@college-de-france.fr.
ORCID
Wayne W. Lukens: 0000-0002-0796-7631
Boris Le Guennic: 0000-0003-3013-0546
Jan Dreiser: 0000-0001-7480-1271
Christophe Copéret: 0000-0001-9660-3890

Author Contributions

O.M., B.L.G., O.C., and C.C. designed and supervised the project. F.A., G.L., and V.M. developed the synthesis and the characterization of the Dy samples and the preparation of the samples for magnetic measurements. W.W.L. recorded the EXAFS data, and the analysis was performed by G.S. and W.W.L. O.C. performed the magnetic measurements. F.A., G.S., B.L.G., J.D., W.W.L., F.P., O.C., V.M., and C.C. wrote the article.

performed at Lawrence Berkeley National Laboratory under Contract No. DE-AC02-05CH11231. Dy L_3-edge XAFS spectra were obtained at the Stanford Synchrotron Radiation Lightsource, SLAC National Accelerator Laboratory, which is supported by the U.S. Department of Energy, Office of Science, Office of Basic Energy Sciences, under Contract No. DE-AC02-76SF00515. O.C., F.P., and B.L.G. thank CNRS, Rennes Métropole, Université de Rennes 1, and the Agence Nationale de la Recherche (Grant No. ANR-13-BS07-0022-01).

Notes

■ ACKNOWLEDGMENTS

■ ABBREVIATIONS

SMM, single-molecule magnet; STM, scanning tunneling microscope; EXAFS, extended X-ray absorption fine structure; XANES, X-ray absorption near edge structure

■ REFERENCES

(1) Sessoli, R.; Gatteschi, D.; Caneschi, A.; Novak, M. A. Magnetic Bistability in a Metal-Ion Cluster. *Nature* **1993**, *365*, 141−143.

(2) Gao, S.; Affronte, M.; Baker, M. L.; Blundell, S.; Bogani, L.; Chibotaru, L. F.; Clérac, R.; Cornia, A.; Coulon, C.; Domingo, N. *Molecular nanomagnets and related phenomena*; Springer: 2015.

(3) Holmberg, R. J.; Murugesu, M. Adhering magnetic molecules to surfaces. *J. Mater. Chem. C* **2015**, *3*, 11986−11998.

(4) Mannini, M.; Sainctavit, P.; Sessoli, R.; Cartier dit Moulin, C.; Pineider, F.; Arrio, M.-A.; Cornia, A.; Gatteschi, D. XAS and XMCD investigation of Mn12 monolayers on gold. *Chem. - Eur. J.* **2008**, *14*, 7530−7535.

(5) Mannini, M.; Pineider, F.; Danieli, C.; Totti, F.; Sorace, L.; Sainctavit, P.; Arrio, M.-A.; Otero, E.; Joly, L.; Cezar, J. C. Quantum tunnelling of the magnetization in a monolayer of oriented single-molecule magnets. *Nature* **2010**, *468*, 417−421.

(6) Holmberg, R. J.; Hutchings, A.-J.; Habib, F.; Korobkov, I.; Scaiano, J. C.; Murugesu, M. Hybrid nanomaterials: anchoring magnetic molecules on naked gold nanocrystals. *Inorg. Chem.* **2013**, *52*, 14411−14418.

(7) Perfetti, M.; Pineider, F.; Poggini, L.; Otero, E.; Mannini, M.; Sorace, L.; Sangregorio, C.; Cornia, A.; Sessoli, R. Grafting single molecule magnets on gold nanoparticles. *Small* **2014**, *10*, 323−329.

(8) Campbell, V. E.; Tonelli, M.; Cimatti, I.; Moussy, J.-B.; Tortech, L.; Dappe, Y. J.; Rivière, E.; Guillot, R.; Delprat, S.; Mattana, R. Engineering the magnetic coupling and anisotropy at the molecule−magnetic surface interface in molecular spintronic devices. *Nat. Commun.* **2016**, *7*, 13646.

(9) Condorelli, G. G.; Motta, A.; Favazza, M.; Nativo, P.; Fragalà, I. L.; Gatteschi, D. Density control of dodecamanganese clusters anchored on silicon (100). *Chem. - Eur. J.* **2006**, *12*, 3558−3566.

(10) Mannini, M.; Bertani, F.; Tudisco, C.; Malavolti, L.; Poggini, L.; Misztal, K.; Menozzi, D.; Motta, A.; Otero, E.; Ohresser, P.; et al. Magnetic behaviour of TbPc2 single-molecule magnets chemically grafted on silicon surface. *Nat. Commun.* **2014**, *5*, 4582.

(11) Kiefl, E.; Mannini, M.; Bernot, K.; Yi, X.; Amato, A.; Leviant, T.; Magnani, A.; Prokscha, T.; Suter, A.; Sessoli, R.; et al. Robust Magnetic Properties of a Sublimable Single-Molecule Magnet. *ACS Nano* **2016**, *10*, 5663−5669.

(12) Wackerlin, C.; Donati, F.; Singha, A.; Baltic, R.; Rusponi, S.; Diller, K.; Patthey, F.; Pivetta, M.; Lan, Y.; Klyatskaya, S.; et al. Giant Hysteresis of Single-Molecule Magnets Adsorbed on a Nonmagnetic Insulator. *Adv. Mater.* **2016**, *28*, 5195−9.

(13) Urdampilleta, M.; Klyatskaya, S.; Cleuziou, J.-P.; Ruben, M.; Wernsdorfer, W. Supramolecular spin valves. *Nat. Mater.* **2011**, *10*, 502−506.

(14) del Carmen Giménez-López, M.; Moro, F.; La Torre, A.; Gómez-García, C. J.; Brown, P. D.; van Slageren, J.; Khlobystov, A. N. Encapsulation of single-molecule magnets in carbon nanotubes. *Nat. Commun.* **2011**, *2*, 407.

(15) Westerström, R.; Uldry, A.-C.; Stania, R.; Dreiser, J.; Piamonteze, C.; Muntwiler, M.; Matsui, F.; Rusponi, S.; Brune, H.; Yang, S.; et al. Surface Aligned Magnetic Moments and Hysteresis of an Endohedral Single-Molecule Magnet on a Metal. *Phys. Rev. Lett.* **2015**, *114*, 087201.

(16) Donati, F.; Rusponi, S.; Stepanow, S.; Wäckerlin, C.; Singha, A.; Persichetti, L.; Baltic, R.; Diller, K.; Patthey, F.; Fernandes, E.; et al. Magnetic remanence in single atoms. *Science* **2016**, *352*, 318−321.

(17) Mathey, L.; Alphazan, T.; Valla, M.; Veyre, L.; Fontaine, H.; Enyedi, V.; Yckache, K.; Danielou, M.; Kerdiles, S.; Guerrero, J.; et al. Functionalization of Silica Nanoparticles and Native Silicon Oxide with Tailored Boron-Molecular Precursors for Efficient and Predictive p-Doping of Silicon. *J. Phys. Chem. C* **2015**, *119*, 13750−13757.

(18) Alphazan, T.; Mathey, L.; Schwarzwälder, M.; Lin, T.-H.; Rossini, A. J.; Wischert, R.; Enyedi, V.; Fontaine, H.; Veillerot, M.; Lesage, A.; et al. Monolayer Doping of Silicon through Grafting a Tailored Molecular Phosphorus Precursor onto Oxide-Passivated Silicon Surfaces. *Chem. Mater.* **2016**, *28*, 3634−3640.

(19) Ishikawa, N.; Sugita, M.; Ishikawa, T.; Koshihara, S.-y.; Kaizu, Y. Lanthanide double-decker complexes functioning as magnets at the single-molecular level. *J. Am. Chem. Soc.* **2003**, *125*, 8694−8695.

(20) Sessoli, R.; Powell, A. K. Strategies towards single molecule magnets based on lanthanide ions. *Coord. Chem. Rev.* **2009**, *253*, 2328−2341.

(21) Harriman, K. L. M.; Murugesu, M. An Organolanthanide Building Block Approach to Single-Molecule Magnets. *Acc. Chem. Res.* **2016**, *49*, 1158−1167.

(22) Lapadula, G.; Bourdolle, A.; Allouche, F.; Conley, M. P.; del Rosal, I.; Maron, L.; Lukens, W. W.; Guyot, Y.; Andraud, C.; Brasselet, S.; et al. Near-IR Two Photon Microscopy Imaging of Silica Nanoparticles Functionalized with Isolated Sensitized Yb(III) Centers. *Chem. Mater.* **2014**, *26*, 1062−1073.

(23) Lapadula, G.; Trummer, D.; Conley, M. P.; Steinmann, M.; Ran, Y. F.; Brasselet, S.; Guyot, Y.; Maury, O.; Decurtins, S.; Liu, S. X.; et al. One-Photon Near-Infrared Sensitization of Well-Defined Yb(III) Surface Complexes for NIR-to-NIR Single Nanoparticle Imaging. *Chem. Mater.* **2015**, *27*, 2033−2039.

(24) Lapadula, G.; Conley, M. P.; Coperet, C.; Andersen, R. A. Synthesis and Characterization of Rare Earth Siloxide Complexes, M[OSi(OtBu)(3)](3)(L)(x) where L is HOSi(OtBu)(3) and x = 0 or 1. *Organometallics* **2015**, *34*, 2271−2277.

(25) Copéret, C.; Comas-Vives, A.; Conley, M. P.; Estes, D. P.; Fedorov, A.; Mougel, V.; Nagae, H.; Núñez-Zarur, F.; Zhizhko, P. A. Surface Organometallic and Coordination Chemistry toward Single-Site Heterogeneous Catalysts: Strategies, Methods, Structures, and Activities. *Chem. Rev.* **2016**, *116*, 323−421.

(26) Rinehart, J. D.; Long, J. R. Exploiting single-ion anisotropy in the design of f-element single-molecule magnets. *Chem. Sci.* **2011**, *2*, 2078−2085.

(27) Terry, K. W.; Lugmair, C. G.; Tilley, T. D. Tris(tert-butoxy)siloxy Complexes as Single-Source Precursors to Homogeneous Zirconia- and Hafnia-Silica Materials. An Alternative to the Sol-Gel Method. *J. Am. Chem. Soc.* **1997**, *119*, 9745−9756.

(28) Fujdala, K. L.; Tilley, T. D. Thermolytic molecular precursor routes to Cr/Si/Al/O and Cr/Si/Zr/O catalysts for the oxidative dehydrogenation and dehydrogenation of propane. *J. Catal.* **2003**, *218*, 123−134.

(29) Conley, M. P.; Delley, M. F.; Siddiqi, G.; Lapadula, G.; Norsic, S.; Monteil, V.; Safonova, O. V.; Copéret, C. Polymerization of Ethylene by Silica-Supported Dinuclear CrIII Sites through an Initiation Step Involving C-H Bond Activation. *Angew. Chem., Int. Ed.* **2014**, *53*, 1872−1876.

(30) Delley, M. F.; Nunez-Zarur, F.; Conley, M. P.; Comas-Vives, A.; Siddiqi, G.; Norsic, S.; Monteil, V.; Safonova, O. V.; Coperet, C. Proton transfers are key elementary steps in ethylene polymerization on isolated chromium(III) silicates. *Proc. Natl. Acad. Sci. U. S. A.* **2014**, *111*, 11624−11629.

(31) Mougel, V.; Chan, K. W.; Siddiqi, G.; Kawakita, K.; Nagae, H.; Tsurugi, H.; Mashima, K.; Safonova, O.; Coperet, C. Low Temperature Activation of Supported Metathesis Catalysts by Organosilicon Reducing Agents. *ACS Cent. Sci.* **2016**, *2*, 569−76.

(32) Hu, Z.; Kaindl, G.; Meyer, G. X-ray absorption near-edge structure at the L I−III thresholds of Pr, Nd, Sm, and Dy compounds with unusual valences. *J. Alloys Compd.* **1997**, *246*, 186−192.

(33) Chen, G.-J.; Gao, C.-Y.; Tian, J.-L.; Tang, J.; Gu, W.; Liu, X.; Yan, S.-P.; Liao, D.-Z.; Cheng, P. Coordination-perturbed single-molecule magnet behaviour of mononuclear dysprosium complexes. *Dalton Trans.* **2011**, *40*, 5579−5583.

(34) The discrepancy between these data is likely due to the low amount of magnetic centers in the samples measured (ca. 0.3 mg per sample).

(35) Woodruff, D. N.; Winpenny, R. E.; Layfield, R. A. Lanthanide single-molecule magnets. *Chem. Rev.* **2013**, *113*, 5110−5148.